



OPEN

Phosphonic acid tagged carbon quantum dots encapsulated in SBA-15 as a novel catalyst for the preparation of *N*-heterocycles with pyrazolo, barbituric acid and indole moieties

Milad Mohammadi Rasooli¹, Hassan Sepehrmansourie¹, Mahmoud Zarei^{2✉},
 Mohammad Ali Zolfigol^{1✉} & Sadegh Rostamnia³

Herein, we have presented a new insight for the synthesis of a hybrid heterogeneous catalyst. For this purpose, phosphonic acid tagged carbon quantum dots of CQDs-N(CH₂PO₃H₂)₂ encapsulated and assembled in channels of SBA-15 using a post-modification strategy. The mesoporous catalyst of functionalized carbon quantum dots (CQDs) was characterized by several techniques. CQDs-N(CH₂PO₃H₂)₂/SBA-15 as an excellent catalyst was applied for the preparation of novel pyrazolo[4',3':5,6]pyrido[2,3-*d*]pyrimidine derivatives by using pyrazole, barbituric acid and indole moieties at 100 °C under the solvent-free condition. The present work shows that a significant increase in the catalytic activity can be achieved by a rational design of mesoporous SBA-15 modified with CQDs for the synthesis of biological active candidates. The synthesized compounds did not convert to their corresponding pyridines via an anomeric-based oxidation mechanism.

In recent years, composite materials have become well-known as a catalyst, absorbent and sensor in modern sciences¹⁻³. The research and development in designing a composite with high selectivity, performance and sensitivity is an urgent need to expand new frontiers of knowledge^{4,5}. Quantum dots based on carbon, nitrogen and graphene as nano-materials with small size 10 nm have exhibited great potential uses in photocatalysis, bio-sensing, heavy metal elements sensing and biomolecule/drug delivery⁶⁻⁹. Despite the success of existing materials and technologies, the stability of CDs especially in harsh chemical and physical conditions and weak thermal stability is still highly desirable. Also, mesoporous silica catalysts are much more functional due to their easy and fast separation from reaction media, which is high surface area, pore volume and tunable pore size¹⁰⁻¹². Besides, a composite material is composed of quantum dots and mesoporous silica as a new property which is investigated as a catalyst, sensor, extraction and determination¹³⁻¹⁶. However, carbon quantum dots (CQDs) encapsulated in the channel of SBA-15 would produce improved or new properties. Therefore, the application of composite materials in the field of catalyst knowledge has a great interest due to their ability to catalyze a wide range of organic synthesis compounds. In this field, we have applied carbon quantum dots (CQDs) and mesoporous silica as a catalyst for the preparation of pyridines, 1,4-dihydropyridines, 4*H*-pyrans and spiropyran compounds¹⁷⁻¹⁹.

Multicomponent reactions (MCRs) as a versatile method have been also of great interest for the preparation of a wide range of *N*-heterocycle compounds with biological activity²⁰⁻²⁹. Therefore, *N*-heterocycles such as 1,4-dihydropyridines (1,4-DHPs) scaffolds make a variety in the drug structures such as Nifedipine (a), Amlodipine (b) and Felodipine (c) (Fig. 1)³⁰⁻³². Also, the biological significance of 1,4-DHPs was investigated in antitumor, anti-ischemic, analgesic, anti-Alzheimer, anti-hypertensive, insecticidal, cardiovascular, anti-inflammatory and anti-microbial conditions³³⁻³⁵. Furthermore, diversity of pyrrole, barbituric acid and indole-based scaffolds

¹Department of Organic Chemistry, Faculty of Chemistry, Bu-Ali Sina University, Hamedan 6517838683, Iran. ²Department of Chemistry, Faculty of Science, University of Qom, Qom 3716146611, Iran. ³Organic and Nano Group (ONG), Department of Chemistry Iran University of Science and Technology (IUST), PO Box 16846-13114, Tehran, Iran. ✉email: mahmoud8103@yahoo.com; zolfi@basu.ac.ir; mzolfigol@yahoo.com

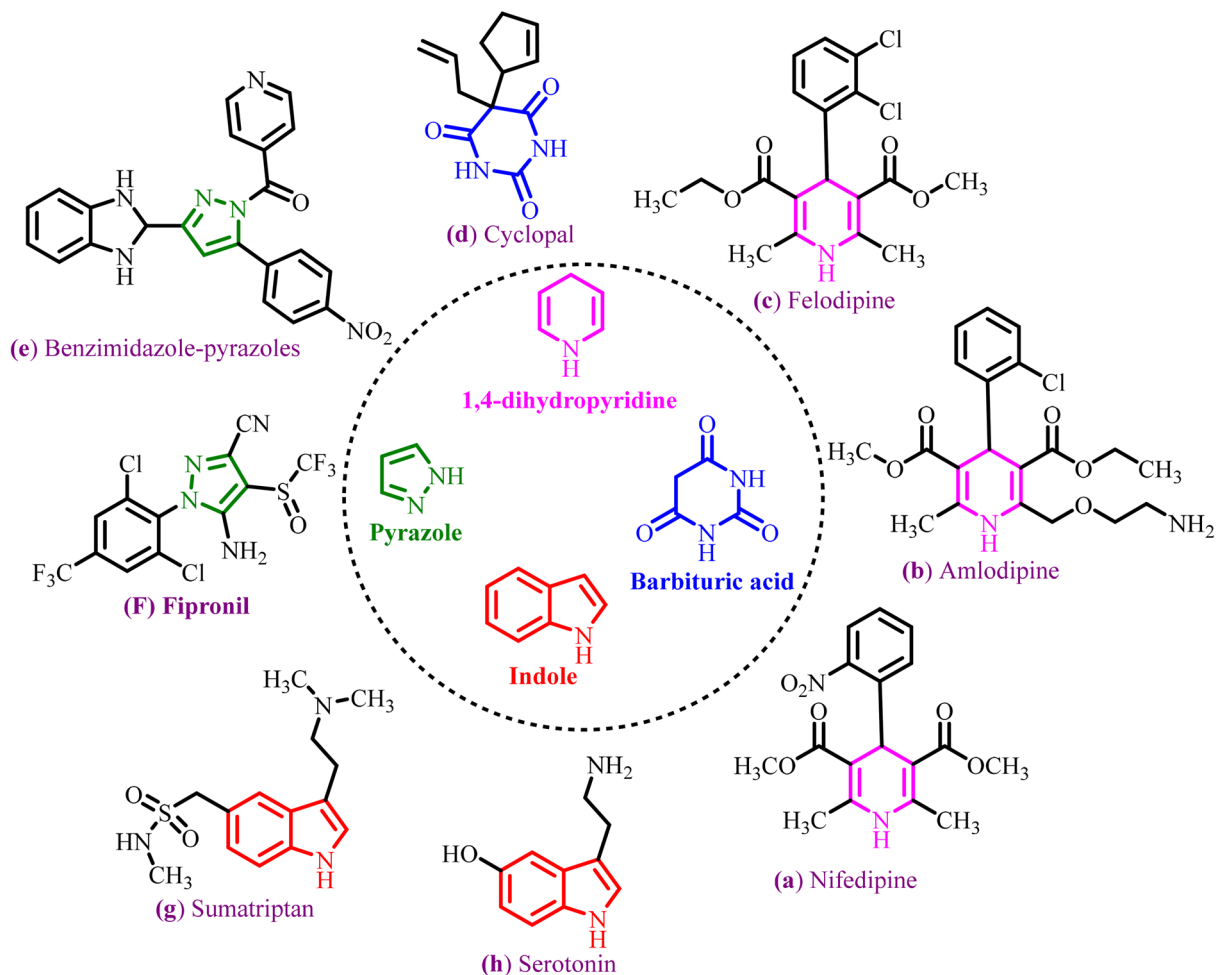


Figure 1. Diversity of pyrrole, barbituric acid and indole based on 1,4-dihydropyridines (1,4-DHPs) structure with biological properties.

such as Cyclopal (d), Benzimidazole-pyrazoles (e), Fipronil (f) Sumatriptan (g) and Serotonin (h) are important in the areas of medicine and agriculture^{36–39}. However, some of these methods are accompanied by restrictions including the use of expensive starting materials, harsh reaction conditions, long reaction times and low yields. Therefore, the development of new, efficient and versatile catalysts is still on demand.

In this strategy, we introduced a convenient method to immobilize phosphonic acid tagged carbon quantum dots (CQDs) in the channels of SBA-15. Then, it was used in the synthesis of *N*-heterocycle compounds with pyrazole, barbituric acid and indole moieties. The novel pyrazolo[4',3':5,6]pyrido[2,3-*d*]pyrimidine derivatives were synthesized in the presence of CQDs- $\text{N}(\text{CH}_2\text{PO}_3\text{H}_2)_2/\text{SBA-15}$ as an excellent mesoporous heterogeneous catalyst (Fig. 2).

Experimental

Synthesis of CQDs- $\text{N}(\text{CH}_2\text{PO}_3\text{H}_2)_2$ and SBA-15. Phosphonic acid tagged carbon quantum dots of CQDs- $\text{N}(\text{CH}_2\text{PO}_3\text{H}_2)_2$ and SBA-15 were synthesized according to our previously reported works^{19,40–44}.

Synthesis of CQDs- $\text{N}(\text{CH}_2\text{PO}_3\text{H}_2)_2/\text{SBA-15}$ composite. For this purpose, in a 100 mL round-bottomed flask, a mixture of CQDs- $\text{N}(\text{CH}_2\text{PO}_3\text{H}_2)_2$ (1 g) and SBA-15 (1 g) and toluene (50 mL) was stirred under reflux conditions for 12 h. After this time, the reaction mixture slowly cooled down to room temperature and participate was separated by a centrifuge (2×4000 rpm). Then, the residual small amount of toluene was evaporated and the brown participate was triturated with EtOH (2×5 mL) and dried under a powerful vacuum at 70 °C. We have synthesized CQDs- $\text{N}(\text{CH}_2\text{PO}_3\text{H}_2)_2/\text{SBA-15}$ composite under the ambient and air atmosphere. Therefore, the environment of the reaction does not affect the synthesis of catalyst.

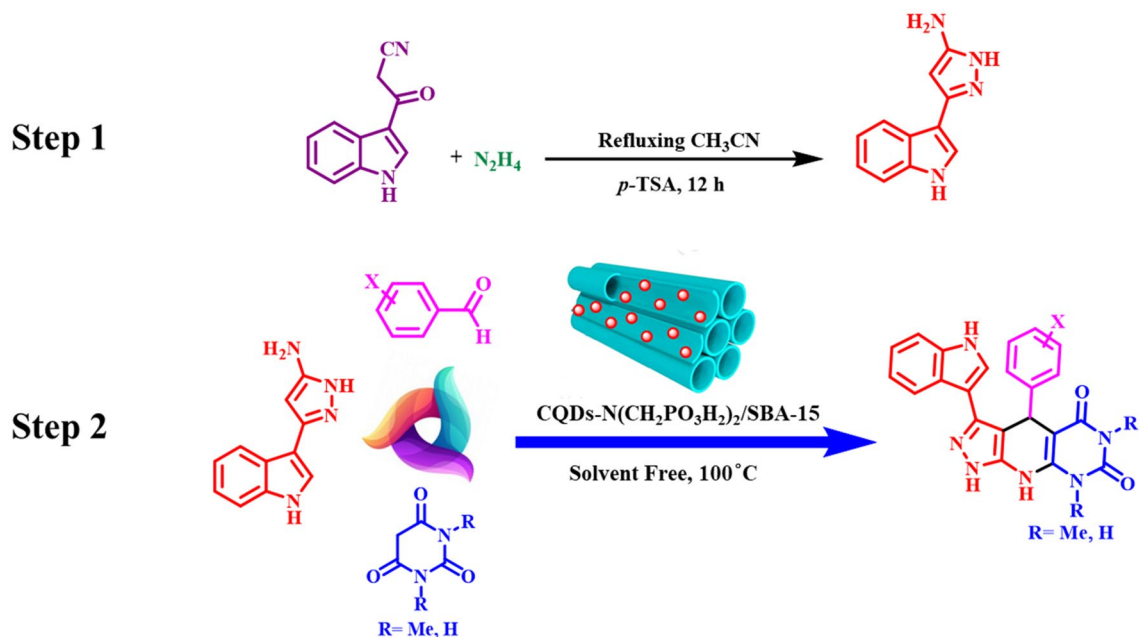


Figure 2. Synthesis of pyrazolo[4',3':5,6]pyrido[2,3-d]pyrimidine derivatives using CQDs- $N(\text{CH}_2\text{PO}_3\text{H}_2)_2$ /SBA-15.

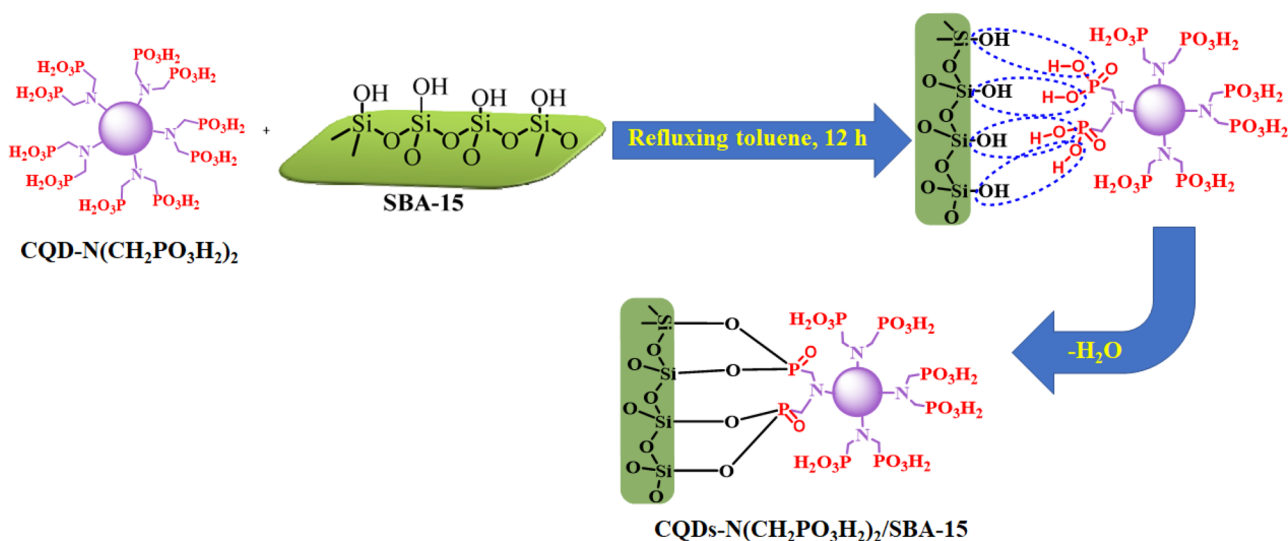


Figure 3. Schematic preparation of CQDs- $N(\text{CH}_2\text{PO}_3\text{H}_2)_2$ /SBA-15 as a desired catalyst.

General procedure for the preparation of *N*-heterocycle compounds with pyrazole barbituric acid and indole tags using CQDs- $N(\text{CH}_2\text{PO}_3\text{H}_2)_2$ /SBA-15. In the first step, the 5-(1*H*-Indol-3-yl)-2*H*-pyrazol-3-ylamine was synthesized according to the procedure reported in the literature (Fig. 2)⁴⁵. In the second step, in a 10 mL round-bottomed flask, a mixture of aldehydes (1 mmol), pyrimidine-2,4,6(1*H*,3*H*,5*H*)-trione derivatives (1 mmol) and as-synthesized 5-(1*H*-indol-3-yl)-1*H*-pyrazol-3-amine (1 mmol) were mixed in the presence of 10 mg of CQDs- $N(\text{CH}_2\text{PO}_3\text{H}_2)_2$ /SBA-15 as a novel heterogeneous catalyst. Then, the mixture temperature was slowly raised up to 100 °C and it was stirred at 100 °C under the solvent-free condition for appropriate time (Tables 2 and 3). After the completion of the reactions which were monitored by the TLC technique, 10 mL of hot EtOH was added to the reaction mixture and the solid catalyst was separated by centrifugation

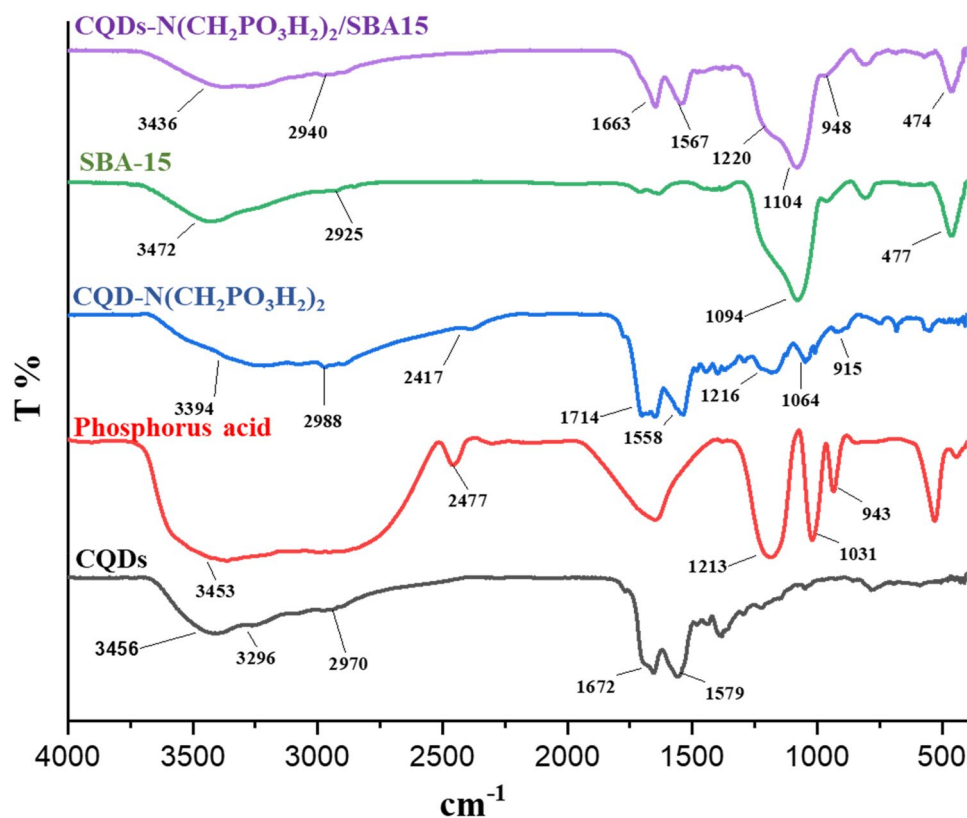


Figure 4. FT-IR spectra of CQDs, phosphorus acid, CQDs-N(CH₂PO₃H₂)₂, SBA-15 and CQDs-N(CH₂PO₃H₂)₂/SBA-15.

(4000 rpm for 10 min). Finally, after the evaporation of the solvent at room temperature, the pure product was obtained and washed with cool ethanol for several times.

Results and discussion

In continuation of our investigation on the mesoporous SBA-15 and CQDs as catalysts in organic synthesis, herein we wish to develop the knowledge of catalysts, consisting of mesoporous SBA-15 and CQDs as highly active composite catalysts^{19,46–48}. With this aim, CQDs-N(CH₂PO₃H₂)₂/SBA-15 as a novel heterogeneous catalyst was synthesized, characterized and applied in the synthesis of target organic molecules (Fig. 3). To determine the structural nature and morphology of the CQDs-N(CH₂PO₃H₂)₂/SBA-15 various techniques such as XRD, SEM, TEM, N₂ adsorption–desorption isotherms, FT-IR, energy dispersive X-ray (EDS) and SEM-elemental mapping were applied.

The FT-IR spectrum of CQDs, phosphorus acid, CQD-N(CH₂PO₃H₂)₂, SBA-15 and CQDs-N(CH₂PO₃H₂)₂/SBA-15 as a desired catalyst were compared in Fig. 4. The broad peak at 2600–3400 cm⁻¹ indicates the OH of PO₃H₂ functional group. The aromatic C-H and C=C stretches bands are, respectively, at 2940 and 1663 cm⁻¹. The absorption bands at 948 and 1058 cm⁻¹ are related to P–O bond stretching and the band at 1104 cm⁻¹ is related to P=O. The peak in the 1714 cm⁻¹ indicates the CO of the carbonyl group in the CQDs-N(CH₂PO₃H₂)₂. Also, the absorption band at 1094 cm⁻¹ was linked to the stretching vibrational of SiO₂ group in the SBA-15. The changes in different stages of synthesis indicated the preparation of the catalyst.

The synthesis of CQDs-N(CH₂PO₃H₂)₂ encapsulated in SBA-15 as a composite material was also checked by XRD patterns of the corresponding starting material components (Figs. 5 and 6). For this purpose, XRD patterns exhibited distinguished three bands inclusive of a sharp band (100) and small bands indexed (110) and (200), which are in a close agreement with the previously reported data¹⁸. As shown in Fig. 5, the broad peak of CQDs-N(CH₂PO₃H₂)₂/SBA-15 corresponds to diffraction lines 002 in carbon quantum dots (CQDs). Therefore, the broad band in 2θ = 15–35° indicated a successful immobilization of CQDs-N(CH₂PO₃H₂)₂ into SBA-15. The textural properties of SBA-15 and CQDs-N(CH₂PO₃H₂)₂/SBA-15 were also studied by N₂ adsorption–desorption isotherms (Fig. 7a,b). A hysteresis loop is observed indicating the presence of mesoporous in the sample. The calculated surface areas for SBA-15 and catalyst based on BET equation and total pore volumes

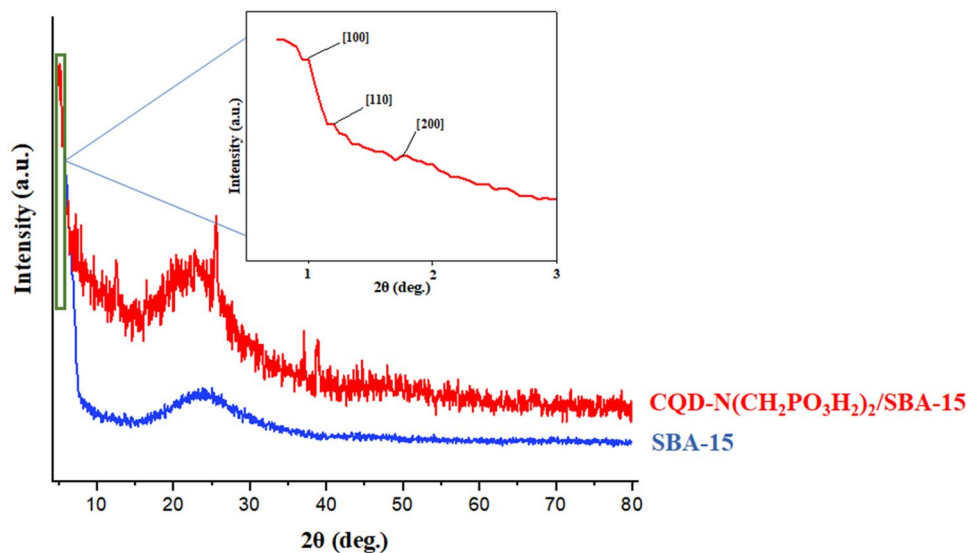


Figure 5. Comparison Low angle and PXRD of CQDs- $\text{N}(\text{CH}_2\text{PO}_3\text{H}_2)_2/\text{SBA-15}$ with SBA-15.

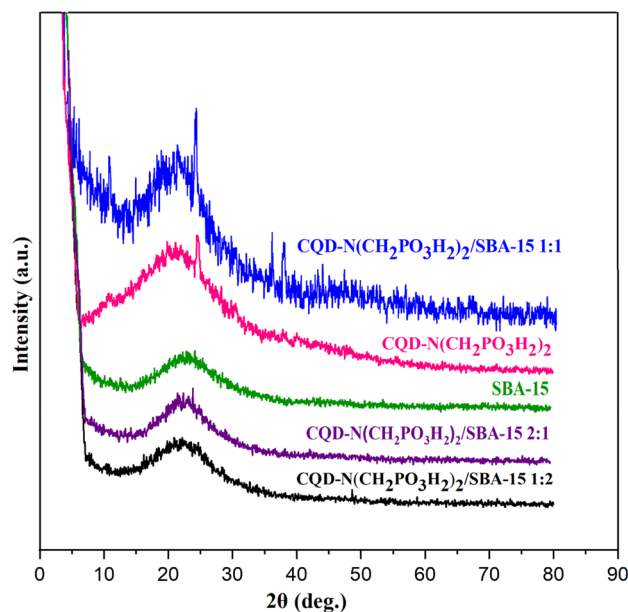


Figure 6. Comparison PXRD of CQDs- $\text{N}(\text{CH}_2\text{PO}_3\text{H}_2)_2/\text{SBA-15}$ (1:1), CQD- $\text{N}(\text{CH}_2\text{PO}_3\text{H}_2)_2$, SBA-15, CQDs- $\text{N}(\text{CH}_2\text{PO}_3\text{H}_2)_2/\text{SBA-15}$ (2:1) and CQDs- $\text{N}(\text{CH}_2\text{PO}_3\text{H}_2)_2/\text{SBA-15}$ (1:2).

are $596.55 \text{ m}^2 \text{ g}^{-1}$, $192.07 \text{ m}^2 \text{ g}^{-1}$ and $0.8564 \text{ cm}^3 \text{ g}^{-1}$, $0.3709 \text{ cm}^3 \text{ g}^{-1}$, respectively. The pore size distribution of CQDs- $\text{N}(\text{CH}_2\text{PO}_3\text{H}_2)_2/\text{SBA15}$ based on BJH method is shown in Fig. 7. This plot clearly shows pores diameter of SBA-15 was 4.03 nm and reached 3.53 in CQDs- $\text{N}(\text{CH}_2\text{PO}_3\text{H}_2)_2/\text{SBA-15}$.

The surface of CQDs- $\text{N}(\text{CH}_2\text{PO}_3\text{H}_2)_2/\text{SBA-15}$ was determined by SEM images (Fig. 8). SEM images of the catalyst revealed that the particles have not completely agglomerated and particles of observed in tubular nano rod shape of silica template (Fig. 8a,b). In another investigation, the scaffold CQDs- $\text{N}(\text{CH}_2\text{PO}_3\text{H}_2)_2/\text{SBA-15}$ is composed of C, N, O, Si and P according to the energy dispersive X-ray spectroscopy (EDX) technique (Fig. 8c). Also, distribution of elements including P (red), Si (blue), O (green), N (yellow) and C (orange) on the surface of the catalyst was investigated and verified by SEM-elemental technique (Fig. 8d). Therefore, energy dispersive X-ray spectroscopy (EDX) and SEM-elemental mapping spectroscopy of all the expected elements confirm the uniform distribution of the elements on the surface.

The morphology and surface of CQDs- $\text{N}(\text{CH}_2\text{PO}_3\text{H}_2)_2/\text{SBA-15}$ was determined by TEM analysis (Fig. 9). The TEM images of the CQDs- $\text{N}(\text{CH}_2\text{PO}_3\text{H}_2)_2/\text{SBA-15}$ were shown to be well fit with the two-dimensional hexagonal meso-structures. Based on these images, the scaffold of mesoporous template has been assembled with carbon

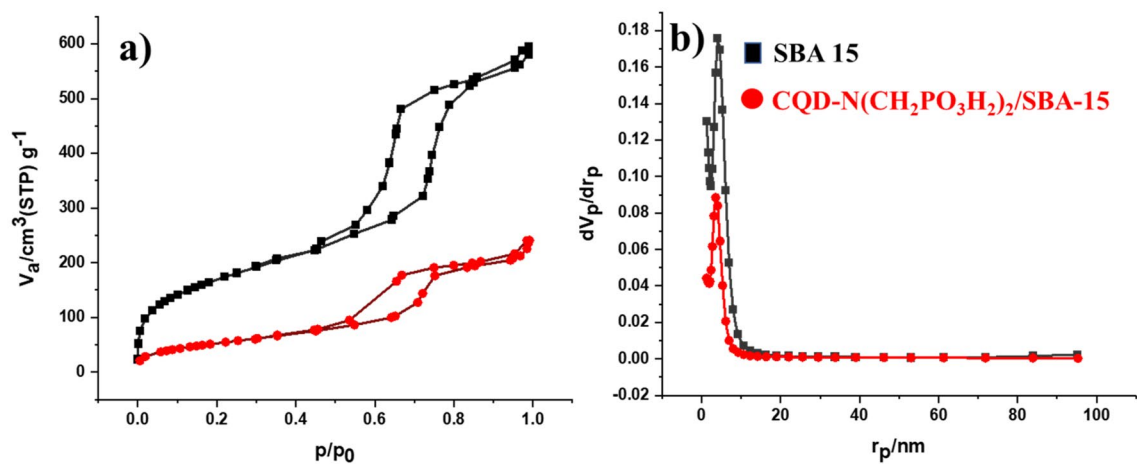


Figure 7. (a) Nitrogen adsorption–desorption isotherm and (b) BJH of SBA-15 and CQDs- $\text{N}(\text{CH}_2\text{PO}_3\text{H}_2)_2/\text{SBA-15}$.

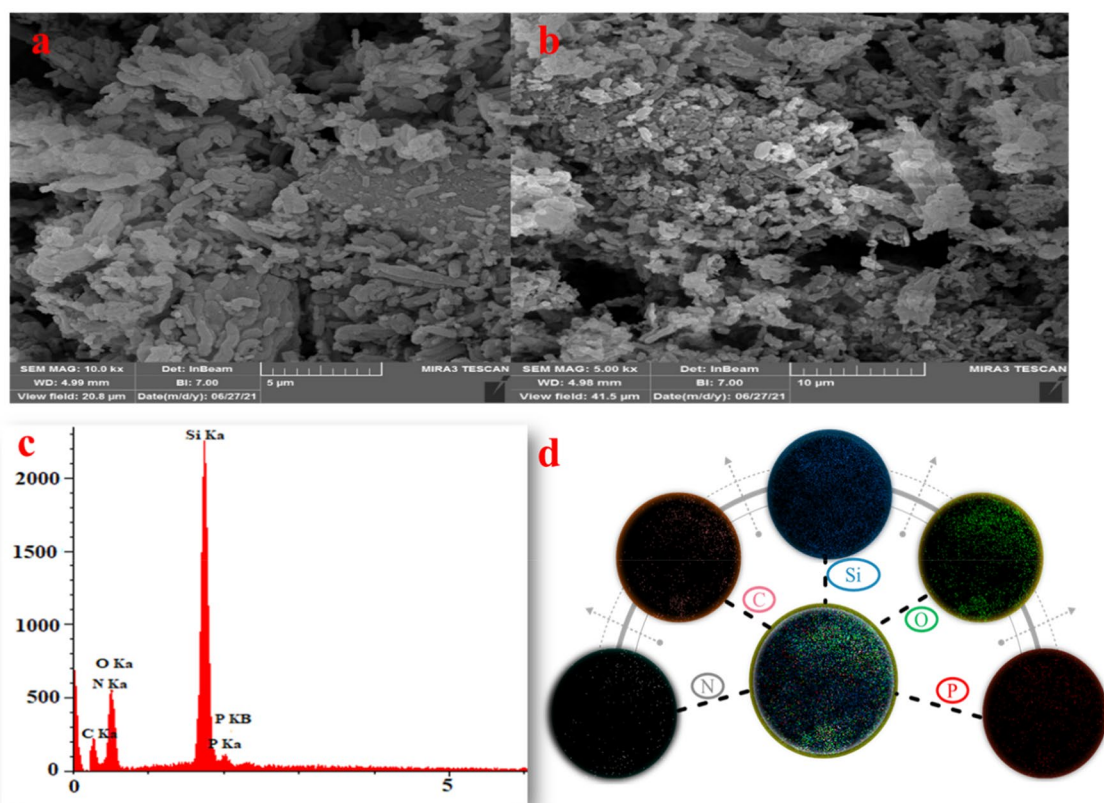


Figure 8. (a,b) Scanning electron microscope (SEM) images of CQDs- $\text{N}(\text{CH}_2\text{PO}_3\text{H}_2)_2/\text{SBA-15}$. (c) Energy dispersive X-ray analysis (EDX) and (d) SEM-elemental technique of CQDs- $\text{N}(\text{CH}_2\text{PO}_3\text{H}_2)_2/\text{SBA-15}$.

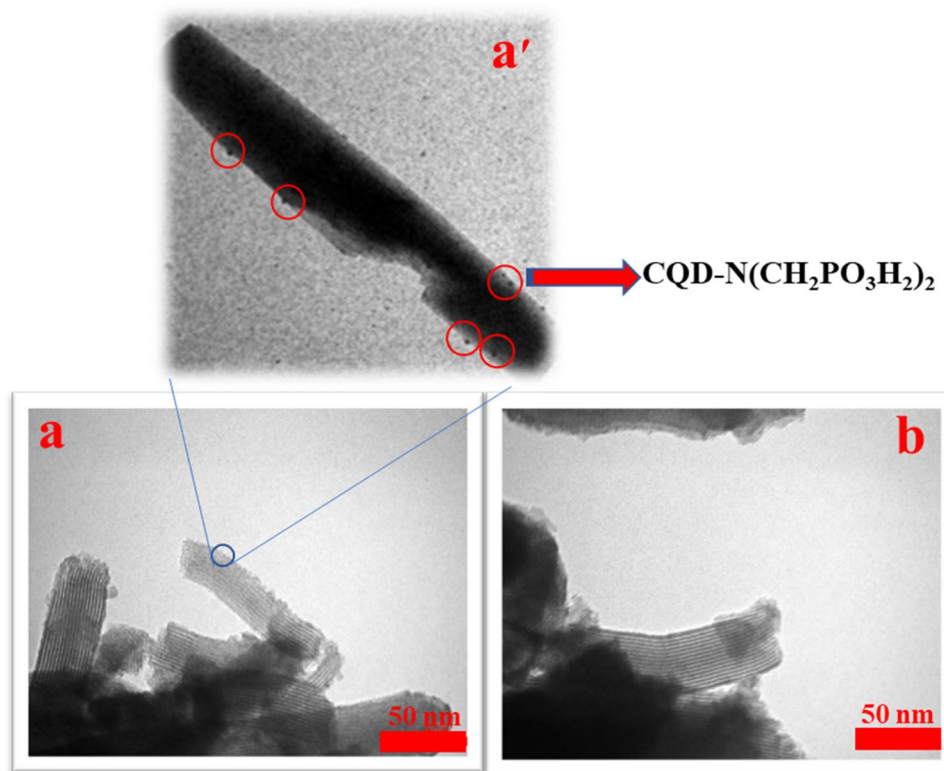


Figure 9. Transmission electron microscopy (TEM) images of CQDs-N(CH₂PO₃H₂)₂/SBA-15.

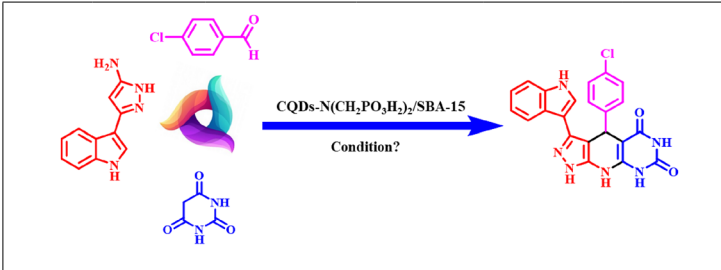
quantum dots (CQDs) (Fig. 9), which agreed well with the results of low-angle XRD and N₂ adsorption–desorption isotherms characterizations.

After successful synthesis and characterization of the CQDs-N(CH₂PO₃H₂)₂/SBA-15, it was used to prepare novel pyrazolo[4',3':5,6]pyrido[2,3-*d*]pyrimidine derivatives. The above-mentioned catalyst was achieved one-pot reaction of between 4-chloro benzaldehyde (1 mmol, 0.14 g), pyrimidine-2,4,6(1*H*,3*H*,5*H*)-trione (1 mmol, 0.128 g) and 5-(1*H*-indol-3-yl)-1*H*-pyrazol-3-amine (1 mmol, 0.198 g) as a model reaction. The model reaction was tested using different amounts of catalysts, solvents and temperatures. The results of the obtained products are summarized in Table 1. The best of choice for the synthesis of novel pyrazolo[4',3':5,6]pyrido[2,3-*d*]pyrimidines was achieved in the presence of catalytic amount of CQDs-N(CH₂PO₃H₂)₂/SBA-15 (10 mg) at 100 °C under the solvent-free condition (Entry 2, Table 1). The model reaction was also tested using different organic solvents such as such EtOH, DMF, H₂O, CH₃CN, *n*-Hexane, CHCl₃, Toluene, MeOH, CH₂Cl₂, EtOAc (5 mL) and water which results of the reaction did not improve) Entry 8–17, Table 1). The results show that CQDs-N(CH₂PO₃H₂)₂/SBA-15 is suitable for the preparation of novel pyrazolo[4',3':5,6]pyrido[2,3-*d*]pyrimidine derivatives.

After the optimization of the reaction conditions, the efficiency and applicability of CQDs-N(CH₂PO₃H₂)₂/SBA-15 were studied for the preparation of novel pyrazolo[4',3':5,6]pyrido[2,3-*d*]pyrimidines. The results are summarized in Tables 2 and 3. As Tables 2 and 3 indicate, pyrimidine-2,4,6(1*H*,3*H*,5*H*)-trione derivatives and 5-(1*H*-indol-3-yl)-1*H*-pyrazol-3-amine as starting materials and various aldehydes including bearing electron-donating, electron-withdrawing and halogens groups afforded desired products (b1–b15), (c1–c7) excellent yields (75–94%) and short reaction times (10–40 min.), respectively.

In a suggested mechanism, the aldehyde is activated by the catalyst. The enol form of the pyrimidine-2,4,6(1*H*,3*H*,5*H*)-trione and activated aldehyde is produced intermediate I. Then, by reaction of intermediate I as a Michael acceptor and 5-(1*H*-indol-3-yl)-1*H*-pyrazol-3-amine leads to the intermediate II. In the following, intermediate II creates intermediate III during the intramolecular reaction and cyclization reaction. Finally, intermediate III loss of molecule H₂O to prepared product (Fig. 10).

In another section, to determine efficiency of CQDs-N(CH₂PO₃H₂)₂/SBA-15 as a catalyst, we have tested the model reaction using previously reported catalysts such as organic, magnetic, solid acid and basic catalysts. The results of the reactions showed that CQDs-N(CH₂PO₃H₂)₂/SBA-15 is the best catalyst for the synthesis of novel pyrazolo[4',3':5,6]pyrido[2,3-*d*]pyrimidine derivatives (short reaction time and high yield) (Table 4). Also, the recyclability and reusability of CQDs-N(CH₂PO₃H₂)₂/SBA-15 as catalyst were also studied on a model reaction



Entry	Solvent	Catalyst (mg)	Temp. (°C)	Time (min.)	Yield (%)
1	–	5	100	40	70
2	–	10	100	15	91
3	–	20	100	35	72
4	–	–	100	120	–
5	–	10	110	20	85
6	–	10	50	60	46
7	–	10	25	70	40
8	EtOH	10	Reflux	45	70
9	DMF	10	100	100	30
10	H ₂ O	10	Reflux	120	–
11	CH ₃ CN	10	Reflux	120	Trace
12	<i>n</i> -Hexane	10	Reflux	120	–
13	CHCl ₃	10	Reflux	100	35
14	Toluene	10	Reflux	120	–
15	MeOH	10	Reflux	60	60
16	CH ₂ Cl ₂	10	Reflux	65	35
17	EtOAc	10	Reflux	120	–

Table 1. Effect of various amounts of catalysts, temperature and solvents in synthesis of pyrazolo[4',3':5,6]pyrido[2,3-*d*]pyrimidines.

under the above-mentioned reaction conditions. The results shown in Fig. 11, CQDs-N(CH₂PO₃H₂)₂/SBA-15 can be reused up to five runs in the reaction without a significant reduction in product yield.

A hot filtration test was conducted to synthesize 1,4-dihydropyridines (1,4-DHPs) as a model reaction under the optimized reaction condition. While running the fresh batch, the catalyst was filtered off at 25 min. At this stage, the reaction yield was 45%. Another reaction was run for 25 min and reaction mixture was filtered off. The filtrate was stirred for another 25 min under the same conditions. Incidentally, the reaction afforded no augmentation in its yield. Therefore, it can be concluded that the structure of the catalyst is not decomposed and the catalyst can be considered a heterogeneous catalyst.

Conclusion

In summary, a novel porous composite catalyst consists of carbon quantum dots (CQDs) and the mesoporous silica namely CQDs-N(CH₂PO₃H₂)₂/SBA-15 was introduced and fully characterized by several techniques. This novel porous catalyst was investigated via a single step reaction for the synthesis of a wide range of novel pyrazolo[4',3':5,6]pyrido[2,3-*d*]pyrimidine derivatives as biological active candidates. The major advantages of described methodology are the high yield of the isolated products, short reaction time, eco-friendly way, mild and green reaction conditions.

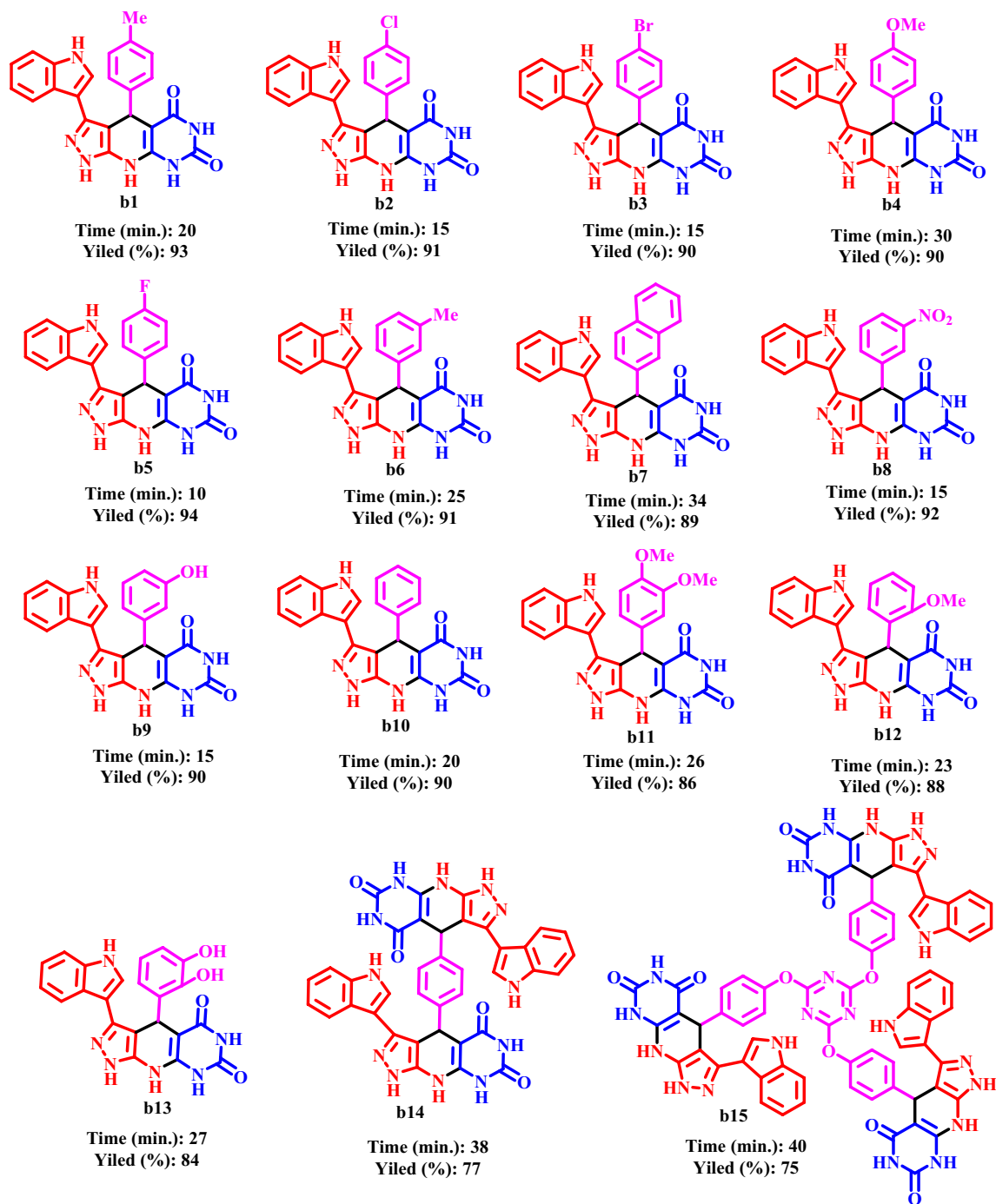


Table 2. Synthesis of pyrazolo[4,3':5,6]pyrido[2,3-*d*]pyrimidines using CQDs- $N(\text{CH}_2\text{PO}_3\text{H}_2)_2/\text{SBA15}$ under solvent free condition.

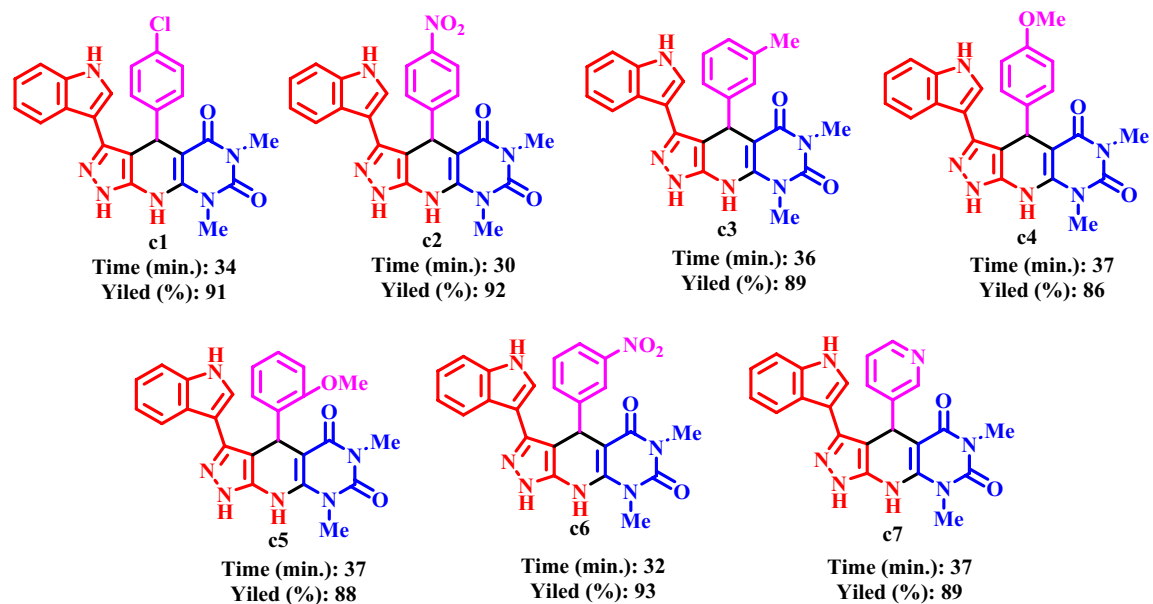


Table 3. Synthesis of pyrazolo[4,3':5,6]pyrido[2,3-*d*]pyrimidines using CQDs-N(CH₂PO₃H₂)₂/SBA15 under solvent free condition.

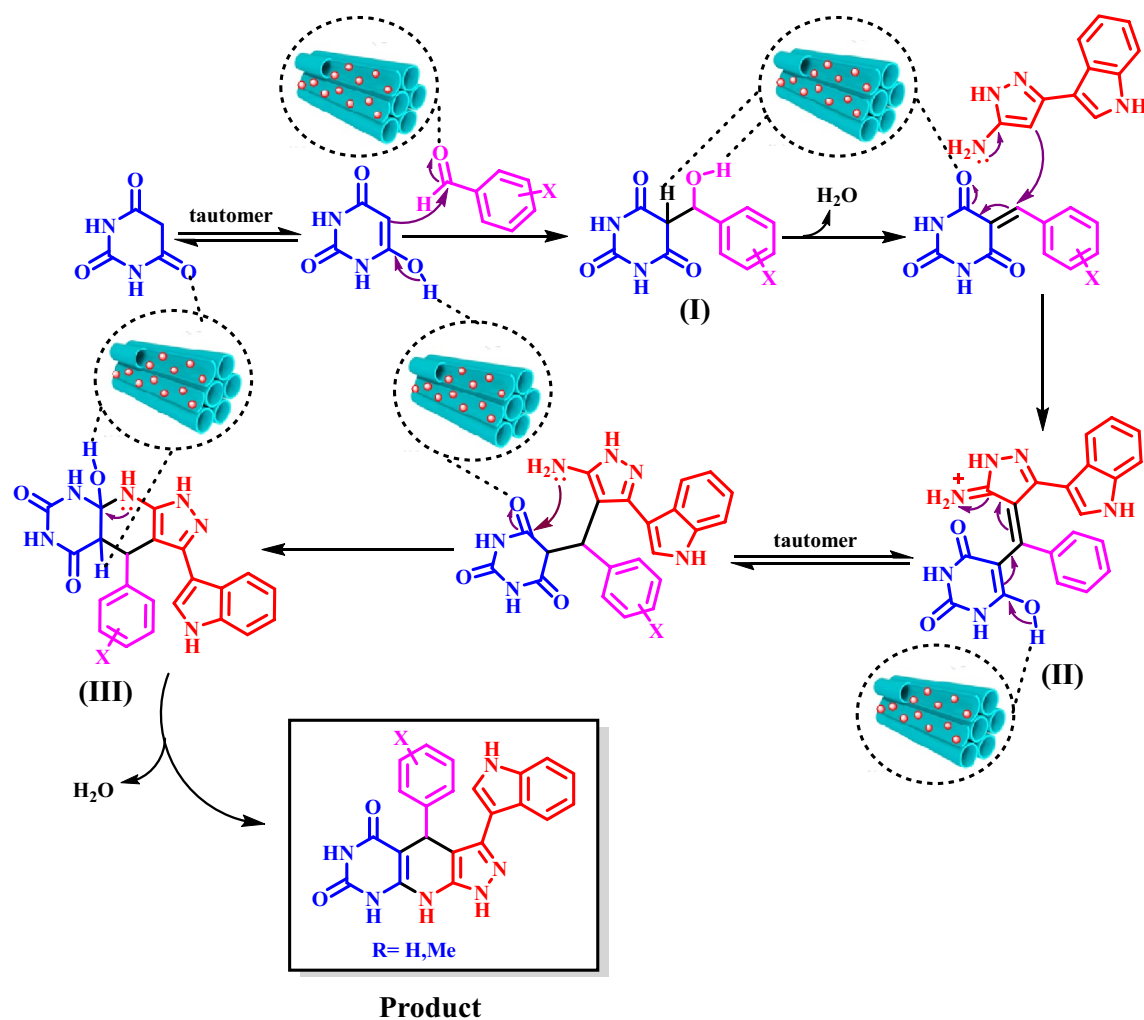
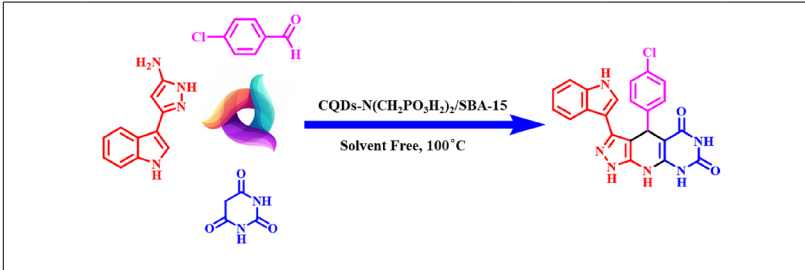


Figure 10. Proposed mechanism for the synthesis of pyrazolo[4,3':5,6]pyrido[2,3-*d*]pyrimidines.



Entry	Catalyst	(mol%)	Time (min.)	Yield (%)
1	FeCl ₃	10	90	20
2	H ₂ SO ₄	10	120	25
3	Fe ₃ O ₄	10 mg	120	Trace
4	NH ₄ NO ₃	10	100	20
5	CF ₃ SO ₃ H	10	80	25
6	GTBSA ²⁹	10	120	20
7	MIL-100(Cr)/NHEtN(CH ₂ PO ₃ H ₂) ₂ ⁴⁹	10	90	45
8	H ₃ [p(W ₃ O ₁₀) ₄].XH ₂ O	10	120	Trace
9	SBA-15/(CH ₂) ₃ N(CH ₂ PO ₃ H ₂)(CH ₂) ₂ -N(CH ₂ PO ₃ H ₂) ₂ ¹⁸	10	60	52
10	[PVI-SO ₃ H]FeCl ₄ ⁵⁰	10	120	30
11	<i>p</i> -TSA	10	120	20
12	SSA ⁵¹	10 mg	100	30
13	Et ₃ N	10	120	–
14	MHMHPA ^{27,28}	10	100	30
15	[Py-SO ₃ H]Cl ⁵²	10	120	20
16	APVPB ⁵³	10 mg	70	40
17	Fe ₃ O ₄ @Co(BDC)-NH ₂ ⁵⁴	10 mg	85	45
18	H ₃ PO ₃	10	70	55
19	CQDs ⁵⁵	10 mg	40	60
20	CQDs-N(CH ₂ PO ₃ H ₂) ₂ ¹⁹	10 mg	30	75
21	CQDs-N(CH ₂ PO ₃ H ₂) ₂ /SBA-15	10 mg	15	91

Table 4. Synthesis of pyrazolo[4',3':5,6]pyrido[2,3-*d*]pyrimidines in the presence of various catalysts.

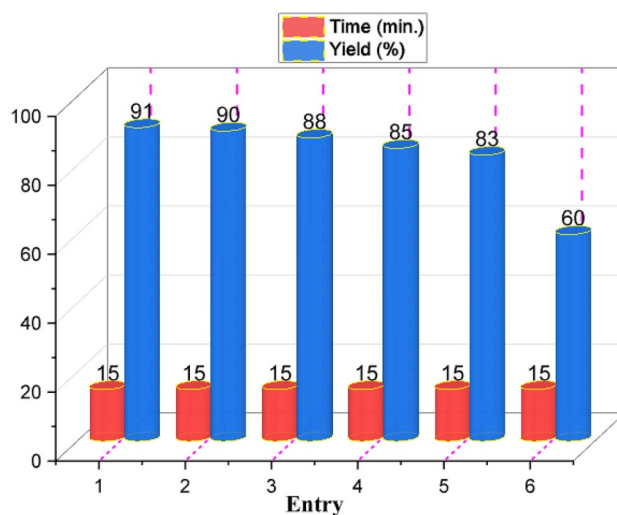


Figure 11. Recyclability of CQDs-N(CH₂PO₃H₂)₂/SBA-15 at the synthesis of pyrazolo[4',3':5,6]pyrido[2,3-*d*]pyrimidines.

Data availability

The datasets used and/or analyzed during the current study available from the corresponding author on reasonable request.

Received: 13 August 2022; Accepted: 16 November 2022

Published online: 02 December 2022

References

- Zhang, Y. *et al.* Ultra-stretchable monofilament flexible sensor with low hysteresis and linearity based on MWCNTs/Ecoflex composite materials. *Macromol. Mater. Eng.* **306**, 2100113 (2021).
- Tiuc, A. E., Nemeş, O., Vermeşan, H. & Toma, A. New sound absorbent composite materials based on sawdust and polyurethane foam. *C. Compos. B. Eng.* **165**, 120–130 (2019).
- Li, X. *et al.* Recent advances in 3D g-C₃N₄ composite photocatalysts for photocatalytic water splitting, degradation of pollutants and CO₂ reduction. *J. Alloys Compd.* **802**, 196–209 (2019).
- Dinu, M. V., Dinu, I. A., Lazar, M. M. & Dragan, E. S. Chitosan-based ion-imprinted cryo-composites with excellent selectivity for copper ions. *Carbohydr. Polym.* **186**, 140–149 (2018).
- Gu, K. *et al.* A facile preparation of positively charged composite nanofiltration membrane with high selectivity and permeability. *J. Membr. Sci.* **581**, 214–223 (2019).
- Su, W. *et al.* Red-emissive carbon quantum dots for nuclear drug delivery in cancer stem cells. *J. Phys. Chem.* **11**, 1357–1363 (2020).
- Wang, Q. *et al.* Single atomically anchored cobalt on carbon quantum dots as efficient photocatalysts for visible light-promoted oxidation reactions. *Chem. Mater.* **32**, 734–743 (2019).
- Algar, W. R. *et al.* Quantum dots as simultaneous acceptors and donors in time-gated Förster resonance energy transfer relays: Characterization and biosensing. *J. Am. Chem. Soc.* **134**, 1876–1891 (2012).
- Zhao, D. L. & Chung, T. S. Applications of carbon quantum dots (CQDs) in membrane technologies: A review. *Water Res.* **147**, 43–49 (2018).
- Linares, N., Silvestre-Albero, A. M., Serrano, E., Silvestre-Albero, J. & García-Martínez, J. Mesoporous materials for clean energy technologies. *Chem. Soc. Rev.* **43**, 7681–7717 (2014).
- Perego, C. & Millini, R. Porous materials in catalysis: Challenges for mesoporous materials. *Chem. Soc. Rev.* **42**, 3956–3976 (2013).
- Zhou, Z. & Hartmann, M. Progress in enzyme immobilization in ordered mesoporous materials and related applications. *Chem. Soc. Rev.* **42**, 3894–3912 (2013).
- Ziarani, G. M., Moradi, R. & Mohajer, F. A. Badieli, 2-Chloroquinoline-3-carbaldehyde modified nanoporous SBA-15-propylamine (SBA-Pr-NCQ) as a selective and sensitive Ag⁺ ion sensor in aqueous media. *J. Phys. Chem. Solids* **161**, 110399 (2022).
- Li, J. *et al.* Largely enhancing luminous efficacy, color-conversion efficiency, and stability for quantum-dot white LEDs using the two-dimensional hexagonal pore structure of SBA-15 mesoporous particles. *ACS Appl. Mater. Interfaces* **11**, 18808–18816 (2019).
- Chang, Q. *et al.* Nitrogen-doped carbon dots encapsulated in the mesoporous channels of SBA-15 with solid-state fluorescence and excellent stability. *Nanoscale* **11**, 7247–7255 (2019).
- Wang, X. *et al.* Determination of 2,4,6-trinitrophenol by in-situ assembly of SBA-15 with multi-hydroxyl carbon dots. *Anal. Chim. Acta.* **1098**, 170–180 (2020).
- Zarei, M., Zolfigol, M. A., Moosavi-Zare, A. R., Noroozadeh, E. & Rostamnia, S. Three-component synthesis of spiropyran using SBA-15/En bonded phosphorous acid [SBA-15/Pr-NH_{1-y}(CH₂PO₃H₂)_y-Et-NH_{2-x}(CH₂PO₃H₂)_x] as a new nanoporous heterogeneous catalyst. *ChemistrySelect* **3**, 12144–12149 (2018).
- Jalili, F., Zarei, M., Zolfigol, M. A., Rostamnia, S. & Moosavi-Zare, A. R. SBA-15/PrN(CH₂PO₃H₂)₂ as a novel and efficient mesoporous solid acid catalyst with phosphorous acid tags and its application on the synthesis of new pyrimido[4,5-*b*]quinolones and pyrido[2,3-*d*]pyrimidines via anomeric based oxidation. *Microporous Mesoporous Mater.* **294**, 109865 (2020).
- Rasooll, M. M. *et al.* Novel nano-architected carbon quantum dots (CQDs) with phosphorous acid tags as an efficient catalyst for the synthesis of multisubstituted 4*H*-pyran with indole moieties under mild conditions. *RSC Adv.* **11**, 25995–26007 (2021).
- Kalhor, S. *et al.* Anodic electro-synthesis of MIL-53(Al)-N(CH₂PO₃H₂)₂ as a mesoporous catalyst for synthesis of novel (*N*-methylpyrrol)-pyrazolo[3,4-*b*]pyridines via a cooperative vinylogous anomeric based oxidation. *Sci. Rep.* **11**, 19370 (2021).
- Babae, S. *et al.* Synthesis of biological based hennotannic acid-based salts over porous bismuth coordination polymer with phosphorous acid tags. *RSC Adv.* **11**, 2141–2157 (2021).
- Tavakoli, E. *et al.* Applications of novel composite UiO-66-NH₂/Melamine with phosphorous acid tags as a porous and efficient catalyst for the preparation of novel spiro-oxindoles. *New J. Chem.* **46**, 19054–19061 (2022).
- Kalhor, S. *et al.* Novel uric acid-based nano organocatalyst with phosphorous acid tags: Application for synthesis of new biologically-interest pyridines with indole moieties via a cooperative vinylogous anomeric based oxidation. *Mol. Catal.* **507**, 111549 (2021).
- Sepehrmansourie, H., Zarei, M., Zolfigol, M. A. & Gu, Y. A new approach for the synthesis of bis (3-Indolyl) pyridines via a cooperative vinylogous anomeric based oxidation using ammonium acetate as a dual reagent-catalyst role under mild and green condition. *Polycycl. Aromat. Compd.* 1–15. <https://doi.org/10.1080/10406638.2022.2128830> (2022).
- Jalili, F., Zarei, M., Zolfigol, M. A. & Khazaei, A. Application of novel metal-organic framework [Zr-UiO-66-PDC-SO₃H]FeCl₄ in the synthesis of dihydrobenzo[*g*]pyrimido[4,5-*b*]quinoline derivatives. *RSC Adv.* **12**, 9058–9068 (2022).
- Naseri, A. M. *et al.* Synthesis and application of [Zr-UiO-66-PDC-SO₃H]Cl MOFs to the preparation of dicyanomethylene pyridines via chemical and electrochemical methods. *Sci. Rep.* **11**, 16817 (2021).
- Afsar, J. *et al.* Synthesis and application of melamine-based nano catalyst with phosphonic acid tags in the synthesis of (3'-indolyl) pyrazolo[3,4-*b*]pyridines via vinylogous anomeric based oxidation. *Mol. Catal.* **482**, 110666 (2020).
- Danishyar, B. *et al.* Synthesis and application of novel magnetic glycoluril tetrakis (methylene phosphorous acid) as a nano biological catalyst for the preparation of nicotinonitriles via a cooperative vinylogous anomeric-based oxidation. *Polycycl. Aromat. Compd.* 1–21. <https://doi.org/10.1080/10406638.2022.2126506> (2022).
- Zarei, M., Sepehrmansourie, H., Zolfigol, M. A., Karamian, R. & Farida, S. H. M. Novel nano-size and crab-like biological-based glycoluril with sulfonic acid tags as a reusable catalyst: Its application to the synthesis of new mono- and bis-spiropyran and their in vitro biological studies. *New J. Chem.* **42**, 14308–14317 (2018).
- Solaimanzadeh, I. Acetazolamide, nifedipine and phosphodiesterase inhibitors: Rationale for their utilization as adjunctive countermeasures in the treatment of coronavirus disease 2019 (COVID-19). *Cureus* **12**, 3 (2019).
- Siddiqi, F. H. *et al.* Felodipine induces autophagy in mouse brains with pharmacokinetics amenable to repurposing. *Nat. Commun.* **10**, 1–14 (2019).
- Solaimanzadeh, I. Nifedipine and amlodipine are associated with improved mortality and decreased risk for intubation and mechanical ventilation in elderly patients hospitalized for COVID-19. *Cureus* **12**, 5 (2020).
- Mishra, A. P., Bajpai, A. & Rai, A. K. 1,4-Dihydropyridine: A dependable heterocyclic ring with the promising and the most anticipable therapeutic effects. *Mini. Rev. Med. Chem.* **19**, 1219–1254 (2019).

34. Gündüz, M. G., Armaković, S. J., Dengiz, C., Tahir, M. N. & Armaković, S. Crystal structure determination and computational studies of 1,4-dihydropyridine derivatives as selective T-type calcium channel blockers. *J. Mol. Struct.* **1230**, 129898 (2021).
35. Taheri-Ledari, R., Rahimi, J. & Maleki, A. Synergistic catalytic effect between ultrasound waves and pyrimidine-2,4-diamine-functionalized magnetic nanoparticles: Applied for synthesis of 1,4-dihydropyridine pharmaceutical derivatives. *Ultrason. Sonochem.* **59**, 104737 (2019).
36. Singh, T. P. & Singh, O. M. Recent progress in biological activities of indole and indole alkaloids. *Mini. Rev. Med. Chem.* **18**, 9–25 (2018).
37. Faria, J. V. *et al.* Recently reported biological activities of pyrazole compounds. *Bioorg. Med. Chem.* **25**, 5891–5903 (2017).
38. Marinescu, M. Synthesis of antimicrobial benzimidazole-pyrazole compounds and their biological activities. *Antibiotics* **10**, 1002 (2021).
39. Moussier, N., Bruche, L., Viani, F. & Zanda, M. Fluorinated barbituric acid derivatives: synthesis and bio-activity. *Curr. Org. Chem.* **7**, 1071–1080 (2003).
40. Rostamnia, S., Doustkhah, E., Golchin Hossieni, H. & Luque, R. Covalently bonded PIDA on SBA-15 as robust Pd support: Water-tolerant designed catalysts for aqueous Suzuki couplings. *ChemistrySelect* **2**, 329–334 (2017).
41. Rostamnia, S. & Doustkhah, E. Covalently bonded zwitterionic sulfamic acid onto the SBA-15 (SBA-15/PrEn-NH₃SO₃H) reveals good Bronsted acidity behavior and catalytic activity in N-formylation of amines. *J. Mol. Catal. A: Chem.* **411**, 317–324 (2016).
42. Doustkhah, E. & Rostamnia, S. Single site supported N-sulfonic acid and N-sulfamate onto SBA-15 for green and sustainable oxidation of sulfides. *Mater. Chem. Phys.* **177**, 229–265 (2016).
43. Rostamnia, S. & Hassankhani, A. Covalently bonded ionic liquid-type sulfamic acid onto SBA-15: SBA-15/NH₃SO₃H as a highly active, reusable, and selective green catalyst for solvent-free synthesis of polyhydroquinolines and dihydropyridines. *Synlett* **25**, 2753–2756 (2014).
44. Rostamnia, S. & Xin, H. Pd(OAc)₂@SBA-15/PrEn nanoreactor: A highly active, reusable and selective phosphine-free catalyst for Suzuki-Miyaura cross-coupling reaction in aqueous media. *Appl. Organometal. Chem.* **27**, 348–352 (2013).
45. El-Mekabaty, A., Etman, H. A. & Mosbah, A. Synthesis of some new fused pyrazole derivatives bearing indole moiety as antioxidant agents. *J. Heterocycl. Chem.* **53**, 894–900 (2016).
46. Doustkhah, E. *et al.* Development of sulfonic-acid-functionalized mesoporous materials: Synthesis and catalytic applications. *Eur. J. Chem.* **25**, 1614–1635 (2019).
47. Dindar, M. H., Yafian, M. R. & Rostamnia, S. Potential of functionalized SBA-15 mesoporous materials for decontamination of water solutions from Cr(VI), As(V) and Hg(II) ions. *J. Environ. Chem. Eng.* **3**, 986–995 (2015).
48. Doustkhah, E. *et al.* Organosiloxane tunability in mesoporous organosilica and punctuated Pd nanoparticles growth; theory and experiment. *Microporous Mesoporous Mater.* **293**, 109832 (2020).
49. Sepehrmansouri, H. *et al.* Multilinker phosphorous acid anchored En/MIL-100(Cr) as a novel nanoporous catalyst for the synthesis of new N-heterocyclic pyrimido[4,5-b]quinolines. *Mol. Catal.* **481**, 110303 (2020).
50. Sepehrmansourie, H., Zarei, M., Taghavi, R. & Zolfigol, M. A. Mesoporous ionically tagged cross-linked poly(vinyl imidazole)s as novel and reusable catalysts for the preparation of N-heterocycle spiroopyrans. *ACS Omega* **4**, 17379–17392 (2019).
51. Zolfigol, M. A. Silica sulfuric acid/NaNO₂ as a novel heterogeneous system for production of thionitrites and disulfides under mild conditions. *Tetrahedron* **57**, 9509–9511 (2001).
52. Moosavi-Zare, A. R., Zolfigol, M. A., Zarei, M., Khakyzadeh, V. & Hasaninejad, A. Design, characterization and application of new ionic liquid 1-sulfonypyridinium chloride as an efficient catalyst for tandem Knoevenagel-Michael reaction of 3-methyl-1-phenyl-1H-pyrazol-5(4H)-one with aldehydes. *Appl. Catal. A Gen.* **467**, 61–68 (2013).
53. Noroozizadeh, E. *et al.* Synthesis of bis-coumarins over acetic acid functionalized poly(4-vinylpyridinium) bromide (APVPB) as a green and efficient catalyst under solvent-free conditions and their biological activity. *J. Iran. Chem. Soc.* **15**, 471–481 (2018).
54. Sepehrmansourie, H., Zarei, M., Zolfigol, M. A., Babae, S. & Rostamnia, S. Application of novel nanomagnetic metal-organic frameworks as a catalyst for the synthesis of new pyridines and 1,4-dihydropyridines via a cooperative vinylogous anomeric based oxidation. *Sci. Rep.* **11**, 5279 (2021).
55. Schneider, J. *et al.* Molecular fluorescence in citric acid-based carbon dots. *J. Phys. Chem. C* **121**, 2014–2022 (2017).

Acknowledgements

We thank the Bu-Ali Sina University and Iran National Science Foundation (INSF) (Grant Number: 98001912) for financial support.

Author contributions

M.M.R. and H.S.; methodology, validation, investigation. M.Z. investigation and writing the original draft. M.A.Z.; supervision, resources, project administration, funding acquisition, conceptualization, writing-review. S.R. writing-review and editing.

Competing interests

The authors declare no competing interests.

Additional information

Supplementary Information The online version contains supplementary material available at <https://doi.org/10.1038/s41598-022-24553-3>.

Correspondence and requests for materials should be addressed to M.Z. or M.A.Z.

Reprints and permissions information is available at www.nature.com/reprints.

Publisher's note Springer Nature remains neutral with regard to jurisdictional claims in published maps and institutional affiliations.



Open Access This article is licensed under a Creative Commons Attribution 4.0 International License, which permits use, sharing, adaptation, distribution and reproduction in any medium or format, as long as you give appropriate credit to the original author(s) and the source, provide a link to the Creative Commons licence, and indicate if changes were made. The images or other third party material in this article are included in the article's Creative Commons licence, unless indicated otherwise in a credit line to the material. If material is not included in the article's Creative Commons licence and your intended use is not permitted by statutory regulation or exceeds the permitted use, you will need to obtain permission directly from the copyright holder. To view a copy of this licence, visit <http://creativecommons.org/licenses/by/4.0/>.

© The Author(s) 2022